De Novo Truncating Mutations in *WASF1* Cause Intellectual Disability with Seizures

Yoko Ito,[1,14] Keren J. Carss,[2,3,14] Sofia T. Duarte,[4] Taila Hartley,[1] Boris Keren,[5] Manju A. Kurian,[6] Isabelle Marey,[5] Perinne Charles,[5] Carla Mendonça,[7] Caroline Nava,[5,8] Rolph Pfundt,[9] Alba Sanchis-Juan,[2,3] Hans van Bokhoven,[9] Anthony van Essen,[10] Conny van Ravenswaaij-Arts,[10] NIHR BioResource, Care4Rare Canada Consortium, Kym M. Boycott,[1,11] Kristin D. Kernohan,[1] Sarah Dyack,[12,15] and F. Lucy Raymond[3,13,15,*]

Next-generation sequencing has been invaluable in the elucidation of the genetic etiology of many subtypes of intellectual disability in recent years. Here, using exome sequencing and whole-genome sequencing, we identified three *de novo* truncating mutations in WAS protein family member 1 (*WASF1*) in five unrelated individuals with moderate to profound intellectual disability with autistic features and seizures. WASF1, also known as WAVE1, is part of the WAVE complex and acts as a mediator between Rac-GTPase and actin to induce actin polymerization. The three mutations connected by Matchmaker Exchange were c.1516C>T (p.Arg506Ter), which occurs in three unrelated individuals, c.1558C>T (p.Gln520Ter), and c.1482delinsGCCAGG (p.Ile494MetfsTer23). All three variants are predicted to partially or fully disrupt the C-terminal actin-binding WCA domain. Functional studies using fibroblast cells from two affected individuals with the c.1516C>T mutation showed a truncated WASF1 and a defect in actin remodeling. This study provides evidence that *de novo* heterozygous mutations in *WASF1* cause a rare form of intellectual disability.

Neurodevelopmental disorders (NDDs), which include intellectual disability (ID), epilepsy, and autism spectrum disorder, are a heterogeneous group of disorders caused by abnormal development of the central nervous system (CNS). The complexity of CNS development is reflected in the fact that over 700 genes to date have been associated with ID, and very few occur at high prevalence.[1,2] Because of the extreme genetic heterogeneity of ID, the utilization of next-generation sequencing (NGS) technology provides an efficient method of determining the genetic cause of ID in individuals and discovering ID-associated genes. In addition, NGS of trios enables detection of *de novo* mutations,[3] including single-nucleotide variants (SNVs) and small indels, which are a major contributing factor to the genetic etiology of moderate to severe ID and NDDs.[4–7]

In this study, we used NGS approaches to identify three *de novo* variants in WAS protein family member 1 (*WASF1* [MIM: 605035]), which encodes WASF1 (also known as WAVE1), in five unrelated individuals with overlapping neurodevelopmental abnormalities, including severe ID with autistic features and seizures. We used Matchmaker Exchange (MME)[8] to connect the four international centers, which had each independently identified *WASF1* as a candidate gene. All three *de novo* variants, including a recurrent truncating variant, cluster within the C-terminal actin-binding WCA domain of WASF1 and are predicted to result in a truncated protein.

The five affected individuals described in this report are from non-consanguineous families and are unrelated. All participants and parents gave informed consent, and the studies were approved by the appropriate institutional research ethics boards (Children's Hospital of Eastern Ontario, Ottawa, Canada; IWK Health Centre, Halifax, Canada; Groupe Hospitalier Pitié-Salpêtrière, Paris, France; East of England Cambridge South, Cambridge, UK; Santa Maria Hospital, Lisbon, Portugal; and Radboud University Medical Center, Nijmegen, the Netherlands [2011-188]). The five affected individuals (P1–P5) have moderate to profound ID with autistic features, seizures, severe impairments in speech, gross motor delay, and a paucity of significant congenital abnormalities. A detailed clinical overview is provided in Table 1. The affected individuals have midfacial hypoplasia but lack a recognizable dysmorphic facial phenotype (Figures S1A–S1D). P5 started walking at 25 months, P1 and P2 began walking at age 3–4 years, and P4 did not walk until age 10 years. P1

[1]Children's Hospital of Eastern Ontario Research Institute, University of Ottawa, Ottawa, ON K1H 8L1 Canada; [2]Department of Haematology, University of Cambridge, Cambridge CB2 0PT, UK; [3]NIHR BioResource, Cambridge University Hospitals NHS Foundation Trust, Cambridge Biomedical Campus, Cambridge CB2 0QQ, UK; [4]Hospital Dona Estefânia, Centro Hospitalar de Lisboa Central, 1169-045 Lisbon, Portugal; [5]Département de Génétique et Centre de Référence Déficiences Intellectuelles de Causes Rares, Hôpital de la Pitié-Salpêtrière, Assistance Publique – Hôpitaux de Paris, 75651 Paris, France; [6]Developmental Neurosciences, Great Ormond Street Institute of Child Health, University College London, London WC1N 1EH, UK; [7]Centro de Neuropediatria e Desenvolvimento, Centro Hospitalar Universitário do Algarve, Faro 8000, Portugal; [8]Sorbonne Universités, Université Pierre et Marie Curie, Paris 75013, France; [9]Department of Human Genetics, Radboudumc, Donders Institute for Brain, Cognition, and Behaviour, Box 9101, 6500 HB Nijmegen, the Netherlands; [10]University of Groningen, University Medical Centre Groningen, Department of Genetics, P.O. Box 30.001, 9700 RB Groningen, the Netherlands; [11]Department of Genetics, Children's Hospital of Eastern Ontario, Ottawa, ON K1H 8L1, Canada; [12]Department of Pediatrics, Dalhousie University, Halifax, NS B3K 6R8, Canada; [13]Department of Medical Genetics, Cambridge Institute for Medical Research, University of Cambridge, Cambridge CB2 0XY, UK
[14]These authors contributed equally to this work
[15]These authors contributed equally to this work
*Correspondence: flr24@cam.ac.uk
https://doi.org/10.1016/j.ajhg.2018.06.001.

Table 1. Key Clinical Features of Affected Individuals

Detail	P1	P2	P3	P4	P5
General					
Age (years)	21	23	23	30	23
Sex	male	male	male	female	male
Birth					
Gestation (weeks)	40	41	39	NR	41
Weight (g)	3,800	4,100	3,370	4,020	4,020
Head circumference (cm)	NR	35.5	35.5	NR	35.5
Neurological					
Intellectual disability	severe to profound	moderate to severe	severe	profound	moderate to severe
Seizures	onset at 8 years; focal with occasional GTC	onset at 6 years; absence and GTC	onset at 8 months; infantile spasms initially, now GTC	onset NR; temporal-lobe epilepsy with partial seizures	none
Speech	single words	simple sentences	non-verbal	NR	single words
Hypotonia	yes	yes	no	yes (axial with hypertonia of extremities)	yes (head control achieved at 11 months)
History of regression	no	no	yes (8 months)	arrested development at age 1 year, 10 months	no
Wide-based gait with poor balance	yes	no	non-ambulant	yes	yes
High pain tolerance	yes	no	yes	possible (automutilation)	yes (automutilation)
Head imaging	MRI: scarce periventricular white matter, enlarged ventricles	MRI: normal	MRI: normal	CT: mild atrophy near Sylvian fissures	MRI: enlarged ventricles
Current Measurements					
Head circumference (cm)	50.4 (<P1; −3.2 SD)	58 (P98; +2 SD)	53.2 (P25; −1.3 SD)	54 (P25; −0.3 SD)	57 (P99; +2.4 SD)
Weight (kg)	40.8 (<P1)	82 (P80)	40.2 (P25)	unknown	65 (P70)
Height (cm)	156.7 (<P1; −2.8 SD)	183 (P80; +1 SD)	168 (P10; −1.2 SD)	150 (P2; −2.8 SD)	175 (P97; +1.8 SD)
Motor Development					
Age at unsupported sitting	18 months	9 months	6 months	22 months	NR
Age at walking	4 years	3 years	non-ambulant	10 years	25 months

(*Continued on next page*)

Table 1. ***Continued***

Detail	P1	P2	P3	P4	P5
Craniofacial					
Midface hypoplasia	yes	yes	no	yes	NR
Eyes	deep set, strabismus, gray sclera	exophthalmia	strabismus, gray sclera	strabismus, vision loss, upslanted palpebral fissures	strabismus
Musculoskleletal					
Joint hyperflexibility	yes	no	no	yes	yes
Ankle valgus	yes	no	no	yes	knee recurvatum
Long tapered fingers	yes	no	yes	no	NR
Feet	narrow, pes planus, short forth toes	short third toes	normal	short, pes planus, short third toes	pes planus
Other					
Nipples	widely spaced	normal	widely spaced	inverted	NR
Café au lait macules	yes	no	yes	no	NR
Feeding problems	trouble sucking, reflux, easy choking	no	cyclic vomiting resolved at age 16 years	no	feeding difficulties, reflux
Genitourinary	no	no	renal stones, recurrent UTIs	small kidneys, mildly dilated pyelum, recurrent UTIs	NR
Constipation	yes	no	yes	yes	yes
HGVSg variant	chr6: g.110422797G>A	chr6: g.110422797G>A	chr6: g.110421847G>A	chr6: g.110422831delinsCCTGGC	chr6: g.110422797G>A
HGVSc variant	c.1516C>T	c.1516C>T	c.1558C>T	c.1482delinsGCCAGG	c.1516C>T
HGVSp variant	p.Arg506Ter	p.Arg506Ter	p.Gln520Ter	p.Ile494MetfsTer23	p.Arg506Ter
Genotype	heterozygous	heterozygous	heterozygous	heterozygous	heterozygous
Inheritance	*de novo*	*de novo*	*de novo*	*de novo*	*de novo*

Abbreviations are as follows: CT, computed tomography; GTC, generalized tonic clonic seizure; MRI, magnetic resonance imaging; NR, not recorded; P, patient; and UTI, urinary tract infection.

requires wheelchair assistance when traveling out of his home. P3 has never achieved independent ambulation. All affected individuals either are non-verbal or have limited speech with a few or single words. All affected individuals except P5 have seizures, although these include a range of seizure types, including generalized and focal seizures; all require antiepileptic therapy. Four of the affected individuals (P1, P2, P4 and P5) had significant hypotonia in infancy, and two (P1 and P4) were described as having a wide-based gait, poor balance, and hyperactivity of movements. Musculoskeletal findings included joint hyperflexibility, ankle valgus, and pes planus in the more severely affected individuals. P5 presented with upper-limb dystonia in the first year of life. A high pain tolerance was observed in P1 and P3, whereas P4 and P5 exhibited automutilation, which is observed in those with an abnormal response to pain. Computed tomography of P1 showed mild atrophy near the Sylvian fissures, magnetic resonance imaging (MRI) of P2 and P3 was normal, and MRI of P4 revealed abnormalities of the periventricular white matter, although this individual also suffered a traumatic birth. MRI of P5 showed enlarged ventricles. Toe abnormalities (short third and fourth toes) were noted in three of the four affected individuals (Figures S1E–S1G). Testing for a range of other genetic conditions was undertaken in the affected individuals but resulted in no alternate diagnoses. Specific gene testing included *MECP2*, *ATRX*, *UBE3A*, *CDKL5*, *MEF2C*, *FOXG1*, *TCF4*, and *NRXN1*, reflecting the differential diagnosis and developmental severity of the condition. All had a normal result on diagnostic microarray testing. Metabolic testing was normal, as was a muscle biopsy of P3.

Because the initial genetic tests were negative, all affected individuals had either exome sequencing or whole-genome sequencing (WGS) performed at their respective centers. Details of the methods used for each affected individual are provided in Table S1. Genomic coordinates throughout this report refer to GRCh37, and coding sequence and protein coordinates refer to the canonical transcript (Ensembl: ENST00000392589; GenBank: NM_003931.2).

Trio exome sequencing was performed on individual P1 and his parents as part of the Care4Rare Canada research program according to our standard approach as previously described.[9] After filtering for rare variants (with a frequency less than 0.1% in gnomAD and present fewer than six times in our in-house controls), all variants in known disease-related genes were assessed, but no variants that could explain this individual's phenotype were identified. In the search for potential novel genes, possible biallelic or X-linked recessive variants were examined, but there were no rare homozygous or hemizygous variants. Compound-heterozygous variants were identified in *CROCC* (MIM: 615776), but this gene was ruled out as a likely candidate because it has many loss-of-function variants in control databases (Table S2). Finally, *de novo* variants in *WASF1*, *ATP5J* (MIM: 603152), *SLC38A4* (MIM: 608065), and *ZNF175* (MIM: 601139) were identified (Table S2). Assessment of protein localization patterns and function and *in silico* mutation predictions determined that *ATP5J*, *SLC38A4*, and *ZNF175* were unlikely to be responsible for this condition (refer to Table S2 for further details). Given the role of WASF1 in actin polymerization and the importance of actin regulation in achieving synaptic plasticity, the *de novo* heterozygous variant in *WASF1* (c.1516C>T [p.Arg506Ter]) was judged to be the strongest candidate for causing this individual's condition and was entered into MME.

Individuals P2 and P5 underwent trio exome sequencing as part of routine diagnostic testing at the Département de Génétique of Hôpital Pitié-Salpêtrière (Paris, France). After filtering for rare variants (with a frequency less than 0.1% in the ExAC Browser), no pathogenic variants, likely pathogenic variants, or variants of unknown significance (VUSs) were identified in known developmental-disease-associated genes. Next, rare variants in genes not previously known to be associated with disease were considered. A heterozygous *de novo* stop-gain variant in *WASF1* (c.1516C>T [p.Arg506Ter]), the same variant identified in P1, was identified in both P2 and P5. A *de novo* missense variant in *CDCA7L* (MIM: 609685) was also identified in P2 but was not considered likely to be pathogenic (Table S2). No additional variants that required consideration of pathogenicity were identified in P5.

Individual P3 and his mother underwent WGS as part of the National Institute for Health Research (NIHR) BioResource study (UK) as previously described.[10] No pathogenic or likely pathogenic variants were found in known developmental-disease-associated genes, but a heterozygous stop-gain variant in *WASF1* (c.1558C>T [p.Gln520Ter]), which was not present in the unaffected mother, was identified. Sanger sequencing of P3 and his parents confirmed that the variant occurs *de novo* in the affected individual (Figure S2B). A hemizygous missense variant in X-linked *ACSL4* (MIM: 300157), in which variants can cause X-linked ID (MIM: 300387), was also identified in P3 and was heterozygous in the mother. This was classified as a VUS because the variant was not previously associated with disease (Table S2).

Individual P4 underwent trio exome sequencing as part of routine diagnostic testing (Groningen, the Netherlands). No pathogenic variants, likely pathogenic variants, or VUSs in known developmental-disease-associated genes were identified. Next, *de novo* variants in genes not previously known to be associated with disease were considered. A heterozygous *de novo* frameshift variant in *WASF1* (c.1482delinsGCCAGG [p.Ile494MetfsTer23]) was identified. No other coding variants that occurred *de novo* were identified.

Initially, the four groups independently identified *WASF1* as a strong candidate because of features consistent with those of developmental-disorder-associated genes. This gene is constrained for loss-of-function variation in the ExAC Browser (pLi = 0.91)[11] and is highly and

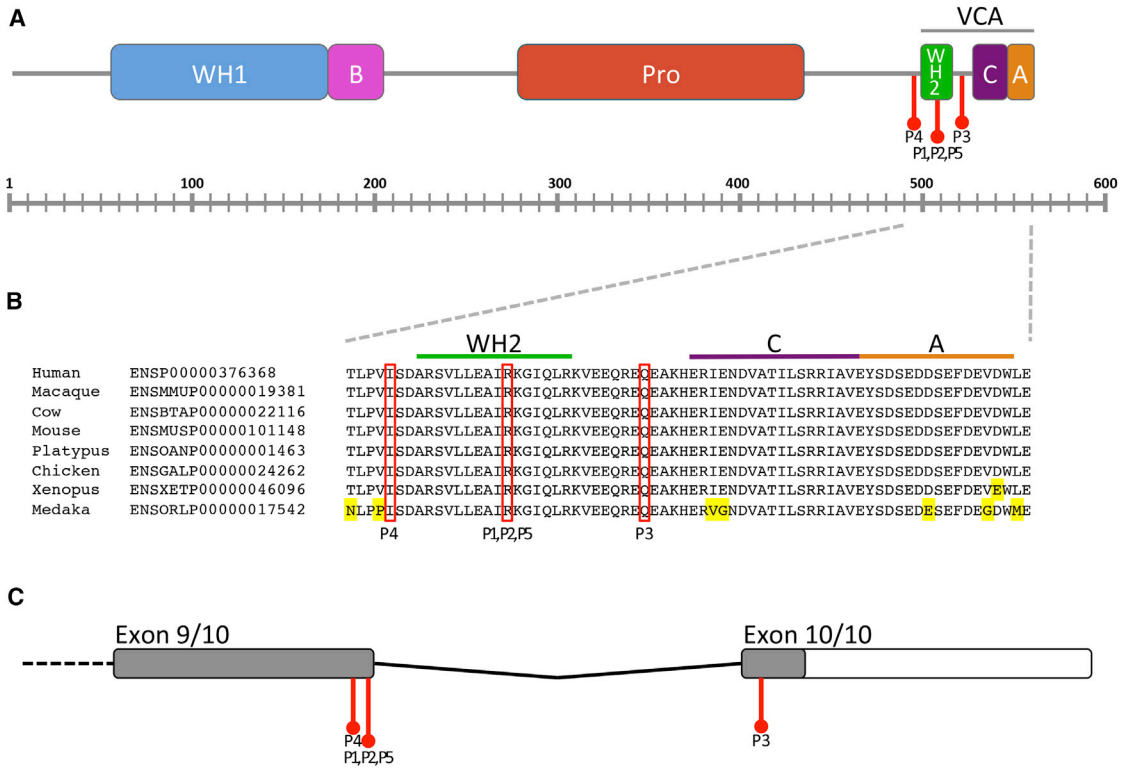

Figure 1. Schematic Diagrams Showing Structure of WASF1 and *WASF1*

(A) Schematic diagram showing full-length WASF1 (also known as WAVE1 [Ensembl: ENSP00000376368]). Variants in the five individuals (indicated in red) cluster around the WH2 domain (domain coordinates are from Stradal et al.[14]). P1, P2, and P5 have p.Arg506Ter, P3 has p.Gln520Ter, and P4 has p.Ile494MetfsTer23. Abbreviations are as follows: WH1, WASP homology 1 domain; B, basic domain; Pro, proline-rich region; WH2, WASP homology 2 domain (also known as the verprolin homology domain); C, cofilin homology domain; A, acidic domain; WCA, collective name for the WH2, C, and A domains.

(B) Schematic diagram showing the amino acid sequence of part of WASF1. The WCA region of WASF1 is conserved throughout evolution. Yellow highlights residues that differ from the human protein sequence.

(C) Schematic diagram showing the 3′ part of *WASF1*, including locations of the participants' variants in red. The gray boxes represent the coding sequence, and the white box represents the 3′ UTR. The variant in P1, P2, and P5 is 6 bps from the end of exon 9 (the penultimate exon). The variant in P4 is 40 bps from the end of exon 9. The variant in P3 is within exon 10 (the final exon).

specifically expressed in the adult human brain.[12] All three *WASF1* variants are absent from 1000 Genomes, the ExAC Browser, and gnomAD.[11,13] The variants in individuals P1 and P3–P5 were confirmed to be *de novo* by Sanger sequencing of the trio (Figure S2B). The read depths for P2 and his mother and father were 127 (with 69 read counts for the alternate allele), 143, and 124, respectively. MME connected three of the groups, and the fourth was connected by personal correspondence with the UK group.

Interestingly, the three *de novo* variants appear to cluster around the WASP-homology 2 (WH2) domain of WASF1 (Figure 1A). A previously published method was used to determine that the clustering is statistically significant ($p = 1.31 \times 10^{-6}$).[15] The C-terminal actin-binding WCA region, which includes the WH2 domain, is highly conserved throughout evolution (Figure 1B). The WCA region plays an important role in regulating WASF1[16,17] so that actin and the Arp2/3 complex can bind to the WCA domain to promote actin polymerization.[18] All three variants identified in the affected individuals fall either within the last 50 bp of the penultimate exon or within the last exon (Figure 1C) and are therefore predicted to result in the generation of a truncated protein that partially or fully eliminates this WCA domain.[19]

Next, the potential effect of the identified *WASF1* variants on protein function was determined. Primary fibroblasts were obtained from individuals P1 and P2, who carry the same c.1516C>T variant (predicted to introduce a premature stop codon at amino acid 506). Amounts of *WASF1* mRNA and WASF1 were examined. Real-time PCR showed variable levels of mRNA between the two affected individuals and control individuals (Figure 2A). For western blot analysis of WASF1, total protein extracts were probed with either a C-terminal antibody (epitope located after amino acid 506; Abcam, ab50356) or an N-terminal antibody (Sigma-Aldrich, W0267) against WASF1. Comparison of control and affected individuals revealed that the cells from affected individuals had both the full-length WASF1 (75 kDa) and a truncated ~70 kDa protein that was not observed in control cells (Figures 2B and 2C). Densitometry quantification of these bands showed that the full-length protein was present at approximately 50% of the

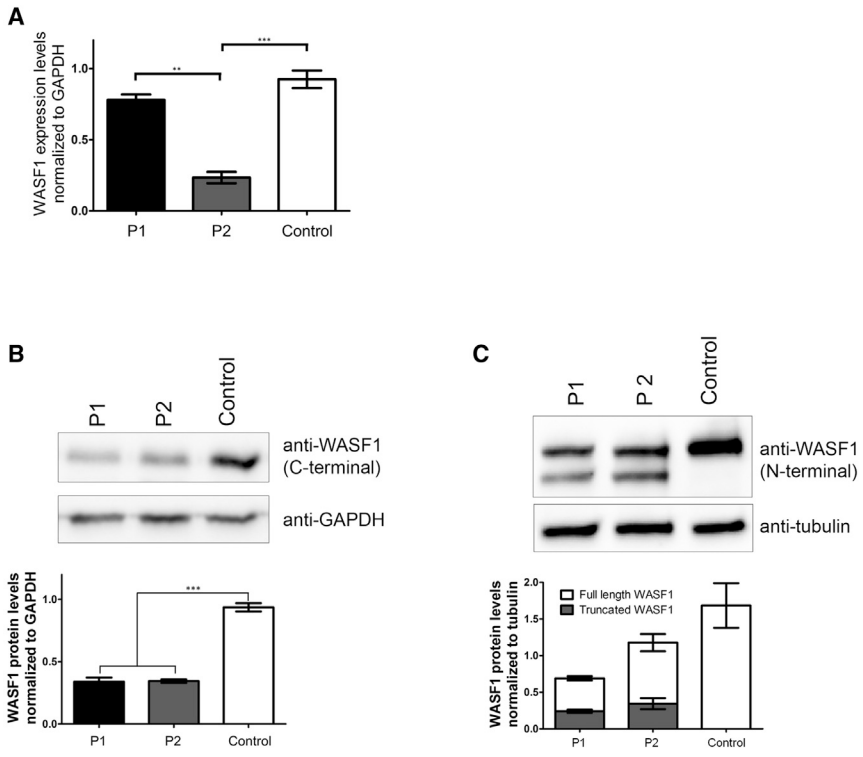

Figure 2. Amounts of *WASF1* mRNA and WASF1 in Fibroblasts Derived from Affected Individuals with the c.1516C>T Variant

(A) RT-qPCR shows variable amounts of *WASF1* mRNA between primary fibroblasts derived from individuals P1 and P2 and healthy control fibroblasts.

(B) Western blot analysis using an antibody with an epitope downstream of Arg506 showed that the amount of full-length WASF1 was approximately 50% lower in affected fibroblasts than in control fibroblasts.

(C) Western blot analysis using an antibody with an epitope in the N-terminal region of WASF1 showed the presence of the full-length and truncated WASF1 in affected fibroblasts. The truncated WASF1 was not present in control fibroblasts. All experiments were performed with fibroblasts derived from three healthy control individuals. Western blots were performed in triplicate, and band intensity was quantified with Image Lab Software (Bio-Rad). Error bars indicate the range of measurement of triplicate samples.

control levels, reflecting the presence of one wild-type allele, whereas the truncated protein was present at 14%–25% of control levels (Figures 2B and 2C). This suggests that although a truncated isoform is produced, it is unstable at either the mRNA or protein level such that the amount of protein is reduced. Therefore, the *WASF1* c.1516C>T variant causes the production of a shorter mutant protein rather than the absence of a protein due to complete nonsense-mediated decay of the primary transcript.

WASF1 plays a critical role in binding actin to initiate actin polymerization. Examination of the reorganization of the actin cytoskeleton during lamellipodia formation in fibroblasts was used for testing this role.[20–22] Serum-starved fibroblasts were trypsinized, re-plated onto poly-L-lysine-coated coverslips, and stimulated with platelet-derived growth factor (PDGF; Sigma-Aldrich, P3201) for inducing the formation of lamellipodia, as previously described.[20] Then cells were fixed, filamentous actin was visualized by labeling with phalloidin (Thermo Fisher Scientific, A12349), and the actin phenotype was quantified in each genotype. In the majority of control cells (77%), actin at the cell periphery formed well-organized, sheet-like lamellipodia structures (Figures 3A and 3B, white arrowhead; Figure S3). This was interspersed with cells in which the actin sheets were interjected by filopodia, which are finger-like actin projections (Figures 3A and 3B, red asterisk; Figure S3). We next assessed fibroblasts from affected individuals and found that although a sheet-like lamellipodia structure was observed along the periphery of 34% and 24% of P1 and P2 cells, respectively, the actin bundles were thinner and less organized than in the control cells (Figures 3A and 3B). We also noted that a portion of cells from P1 and P2 had severe disruptions in actin organization such that no lamellipodia delineated the cell periphery and only filopodial projections were present (12% and 11% for P1 and P2, respectively; Figures 3A and 3B). This phenotype was not seen in control cells. Therefore, cells from affected individuals have an alteration in actin organization, suggesting that the presence of a truncated WASF1 results in defective actin remodeling during the formation of lamellipodia.

Finally, WASF1-dependent actin polymerization has been shown to mediate mitochondrial trafficking into dendritic spines in primary neurons;[23] therefore, we assessed mitochondrial morphology in fibroblasts with the c.1516C>T variant. Mitochondria were visualized and the average length was quantified as previously described.[24] As expected, a dense and complex network of mitochondria was present in both control and affected fibroblasts. Quantification revealed that mitochondria in the cells from affected individuals were significantly longer than those in control fibroblasts (Figure 3C). This result suggests that the presence of the c.1516C>T variant in *WASF1* disrupts the regulation of mitochondrial dynamics and alters the normal balance between fission and fusion in affected fibroblasts.

This report provides evidence that *de novo* truncating variants in *WASF1* in five unrelated individuals cause a NDD comprising severe ID with autistic features, seizures, and developmental delay. Interestingly, three of the five individuals in this study have the same *de novo* variant

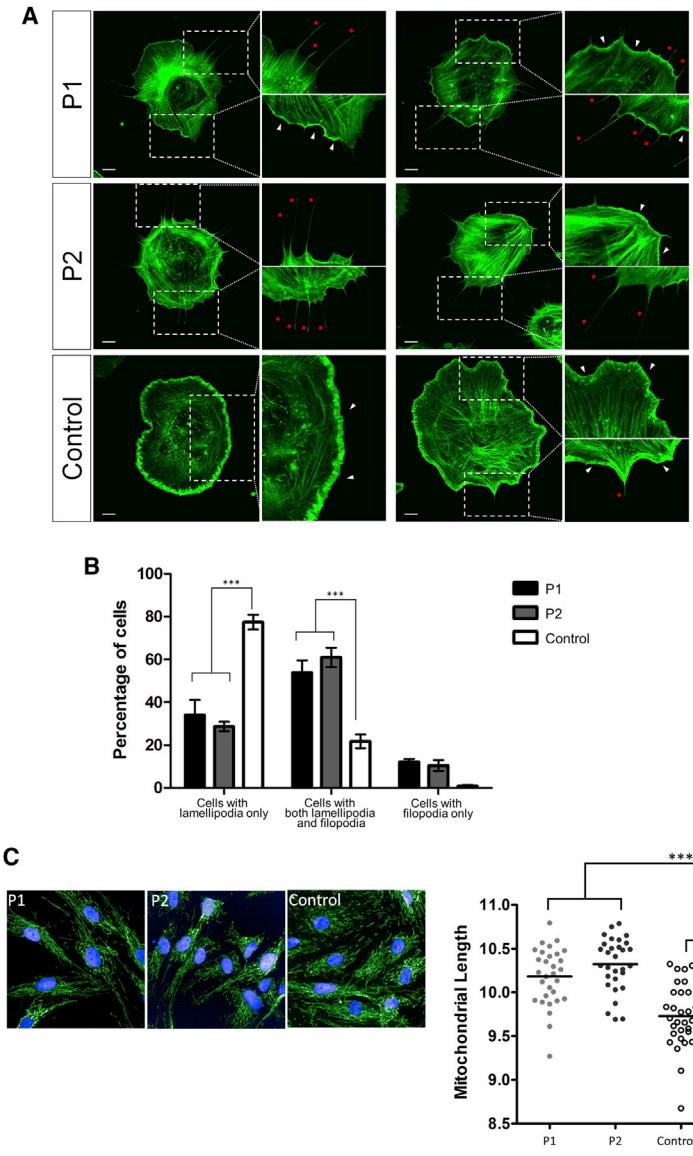

Figure 3. Lamellipodia Formation and Mitochondrial Morphology in Fibroblasts Derived from Individuals with the c.1516C>T Variant

(A) Primary fibroblasts were treated with PDGF for inducing the formation of lamellipodia. Visualization of the filamentous actin by phalloidin staining revealed the disruption of actin in the cell periphery of P1 and P2 fibroblasts. In the insets, lamellipodia and filopodia are marked by white arrowheads and red asterisks, respectively. Scale bars represent 10 μm.

(B) Cells were categorized into three groups on the basis of the predominant actin phenotype present: cells displaying lamellipodia only, cells displaying a mixture of lamellipodia and filopodia, and cells displaying filopodia only. Quantification based on these three categories indicates that significantly fewer affected fibroblasts than control fibroblasts are able to form solely lamellipodia.

(C) Confocal microscopic analysis of TOMM-20-immunostained mitochondria (in green) indicated that both affected fibroblasts have significantly elongated mitochondria. The nuclei were visualized by DAPI staining (in blue).

(c.1516C>T [Ensembl: ENST00000392589]). Three of the four individuals have VUSs in other genes in addition to the *WASF1* variants. Population-level sequencing initiatives have enabled increased recognition of the prevalence of recurrent benign *de novo* mutations.[25] Although it is unlikely, the possibility that they contribute to the respective individuals' phenotypes cannot be excluded.

The variants described as associated with this NDD are all stop-gain or frameshift variants and significantly cluster around the C-terminal WH2 domain in the WCA region of WASF1. The truncated protein observed for c.1516C>T (p.Arg506Ter) suggests that all three variants are likely to lead to altered function of the mutant protein rather than complete protein loss or haploinsufficiency from degradation through nonsense-mediated decay. In a disease context, recurrent *de novo* events are known to be associated with specific dominant-negative or gain-of-function effects, such as *FGFR3* (MIM: 134934) variants causing achondroplasia (MIM: 100800), and are usually missense variants.[26] Clustering and recurrence of *de novo* protein-truncating mutations also do occur, albeit less frequently because the genic localization of a pathogenic mutation resulting in haploinsufficiency is generally not critical.[15,27,28] Additional individuals with rare *WASF1* variants are required for determining whether any pathogenic variants lie outside of this WCA region and/or whether a spectrum of phenotypes is perhaps associated with different variants in this gene.

WASF1 is an essential component of the actin pathway where RAC1 activation triggers a conformational change in WASF1 to allow binding of actin and ARP2/3 to the WCA domain to initiate actin polymerization.[20,21,29,30] The presence of a truncated protein that lacks the WCA region, as observed here, most likely disrupts the WASF1 complex itself, its interactions with CYFIP1, its proteasomal degradation, and the binding of actin (Figure 2C).[16,17,31] Like mutations in *WASF1*, mutations in *RAC1* similarly disrupt the formation of lamellipodia in fibroblasts,[32] indicating that the organization and stabilization of actin bundles during the formation of lamellipodia is likely to be compromised by truncated WASF1.

WASF1-dependent actin polymerization is known to be important in CNS development and synaptic plasticity.[18,33–39] Two different *WASF1*-null mouse models demonstrate cognitive impairments, including deficits in

sensorimotor function, learning, and memory.[12,40] In addition, mutations in a number of genes in the actin regulatory pathway, namely, formin 2 (*FMN2* [MIM: 606373]),[41] actin gamma-1 (*ACTG1* [MIM: 102560]),[42] rho guanine nucleotide exchange factor 6 (*ARHGEF6* [MIM: 300267]),[43,44] and RAS-related C3 botulinum toxin substrate 1 (*RAC1* [MIM: 602048]),[32] are associated with ID.

WASF1 localizes to the outer mitochondrial membrane, where it has been shown to play a role in the trafficking of mitochondria to the dendritic spines.[23,44,45] Actin itself has also been shown to be necessary for mediating mitochondrial fission.[45] Given that fibroblasts derived from affected individuals with the c.1516C>T variant show elongated mitochondria (Figure 3C), WASF1 most likely plays additional roles in regulating mitochondrial dynamics, although how variants in *WASF1* affect mitochondrial function in affected individuals remains to be elucidated.

In summary, *de novo* heterozygous truncating variants in *WASF1* cause a NDD in individuals with ID associated with autistic features, seizures, and developmental delay. The three *de novo* variants, identified in five unrelated affected individuals, are all predicted to affect the actin-binding C-terminal WCA region of WASF1. The clustering of truncating pathogenic variants reported here and the presence of a truncated protein in cells from affected individuals imply either a gain-of-function or dominant-negative mechanism of disease. Because WASF1 functions within a large protein complex with ABI2, CYFIP1 or CYFIP2, BRK1, and NCKAP1, the hypothesis that these variants have a most likely dominant-negative effect remains to be tested. This study further expands the list of actin-regulatory-pathway genes associated with NDD and demonstrates the value of sharing genomic data through MME to identify the consequence of extremely rare mutational events.

Supplemental Data

Supplemental Data include three figures and two tables and can be found with this article online at https://doi.org/10.1016/j.ajhg.2018.06.001.

Consortia

The NIHR BioResource consists of Timothy Aitman, David Bennett, Mark Caulfield, Patrick Chinnery, Daniel Gale, Ania Koziell, Taco W. Kuijpers, Michael A. Laffan, Eamonn Maher, Hugh S. Markus, Nicholas W. Morrell, Willem H. Ouwehand, David J. Perry, F. Lucy Raymond, Irene Roberts, Kenneth G.C. Smith, Adrian Thrasher, Hugh Watkins, Catherine Williamson, Geoffrey Woods, Sofie Ashford, John R. Bradley, Debra Fletcher, Tracey Hammerton, Roger James, Nathalie Kingston, Christopher J. Penkett, Kathleen Stirrups, Marijke Veltman, Tim Young, Matthew Brown, Naomi Clements-Brod, John Davis, Eleanor Dewhurst, Helen Dolling, Marie Erwood, Amy Frary, Rachel Linger, Jennifer M. Martin, Sofia Papadia, Karola Rehnstrom, Hannah Stark, David Allsup, Steve Austin, Tamam Bakchoul, Tadbir K. Bariana, Paula Bolton-Maggs, Elizabeth Chalmers, Janine Collins, Peter Collins, Wendy N. Erber, Tamara Everington, Remi Favier, Kathleen Freson, Bruce Furie, Michael Gattens, Johanna Gebhart, Keith Gomez, Daniel Greene, Andreas Greinacher, Paolo Gresele, Daniel Hart, Johan W.M. Heemskerk, Yvonne Henskens, Rashid Kazmi, David Keeling, Anne M. Kelly, Michele P. Lambert, Claire Lentaigne, Ri Liesner, Mike Makris, Sarah Mangles, Mary Mathias, Carolyn M. Millar, Andrew Mumford, Paquita Nurden, Jeanette Payne, John Pasi, Katheljne Peerlinck, Shoshana Revel-Vilk, Michael Richards, Matthew Rondina, Catherine Roughley, Sol Schulman, Harald Schulze, Marie Scully, Suthesh Sivapalaratnam, Matthew Stubbs, R. Campbell Tait, Kate Talks, Jecko Thachil, Cheng-Hock Toh, Ernest Turro, Chris Van Geet, Minka De Vries, Timothy Q. Warner, Henry Watson, Sarah Westbury, Abigail Furnell, Rutendo Mapeta, Paula Rayner-Matthews, Ilenia Simeoni, Simon Staines, Jonathan Stephens, Christopher Watt, Deborah Whitehorn, Antony Attwood, Louise Daugherty, Sri V.V. Deevi, Csaba Halmagyi, Fengyuan Hu, Vera Matser, Stuart Meacham, Karyn Megy, Olga Shamardina, Catherine Titterton, Salih Tuna, Ping Yu, Julie von Ziegenweldt, William Astle, Marta Bleda, Keren J. Carss, Stefan Gräf, Matthias Haimel, Hana Lango-Allen, Sylvia Richardson, Paul Calleja, Stuart Rankin, Wojciech Turek, Julie Anderson, Christine Bryson, Jenny Carmichael, Coleen McJannet, Sophie Stock, Louise Allen, Gautum Ambegaonkar, Ruth Armstrong, Gavin Arno, Maria Bitner-Glindzicz, Angie Brady, Natalie Canham, Manali Chitre, Emma Clement, Virginia Clowes, Patrick Deegan, Charu Deshpande, Rainer Doffinger, Helen Firth, Frances Flinter, Courtney French, Alice Gardham, Neeti Ghali, Paul Gissen, Detelina Grozeva, Robert Henderson, Anke Hensiek, Simon Holden, Muriel Holder, Susan Holder, Jane Hurst, Dragana Josifova, Deepa Krishnakumar, Manju A. Kurian, Melissa Lees, Robert MacLaren, Anna Maw, Sarju Mehta, Michel Michaelides, Anthony Moore, Elaine Murphy, Soo-Mi Park, Alasdair Parker, Chris Patch, Joan Paterson, Julia Rankin, Evan Reid, Elisabeth Rosser, Alba Sanchis-Juan, Richard Sandford, Saikat Santra, Richard Scott, Aman Sohal, Penelope Stein, Ellen Thomas, Dorothy Thompson, Marc Tischkowitz, Julie Vogt, Emma Wakeling, Evangeline Wassmer, Andrew Webster, Sonia Ali, Souad Ali, Harm J. Boggard, Colin Church, Gerry Coghlan, Victoria Cookson, Paul A. Corris, Amanda Creaser-Myers, Rosa DaCosta, Natalie Dormand, Mélanie Eyries, Henning Gall, Pavandeep K. Ghataorhe, Stefano Ghio, Ardi Ghofrani, J. Simon R. Gibbs, Barbara Girerd, Alan Greenhalgh, Charaka Hadinnapola, Arjan C. Houweling, Marc Humbert, Anna Huis in't Veld, Fiona Kennedy, David G. Kiely, Gabor Kovacs, Allan Lawrie, Rob V. Mackenzie Ross, Rajiv Machado, Larahmie Masati, Sharon Meehan, Shahin Moledina, David Montani, Shokri Othman, Andrew J. Peacock, Joanna Pepke-Zaba, Val Pollock, Gary Polwarth, Lavanya Ranganathan, Christopher J. Rhodes, Kevin Rue-Albrecht, Gwen Schotte, Debbie Shipley, Florent Soubrier, Laura Southgate, Laura Scelsi, Jay Suntharalingam, Yvonne Tan, Mark Toshner, Carmen M. Treacy, Richard Trembath, Anton Vonk Noordegraaf, Sara Walker, Ivy Wanjiku, John Wharton, Martin Wilkins, Stephen J. Wort, Katherine Yates, Hana Alachkar, Richard Antrobus, Gururaj Arumugakani, Chiara Bacchelli, Helen Baxendale, Claire Bethune, Shahnaz Bibi, Claire Booth, Michael Browning, Siobhan Burns, Anita Chandra, Nichola Cooper, Sophie Davies, Lisa Devlin, Elizabeth Drewe, David Edgar, William Egner, Rohit Ghurye, Kimberley Gilmour, Sarah Goddard, Pavel Gordins, Sofia Grigoriadou, Scott Hackett, Rosie Hague, Lorraine Harper, Grant Hayman, Archana Herwadkar, Aarnoud Huissoon, Stephen Jolles, Peter Kelleher, Dinakantha Kumararatne, Sara Lear, Hilary Longhurst, Lorena Lorenzo, Jesmeen Maimaris, Ania Manson, Elizabeth McDermott, Sai

Murng, Sergey Nejentsev, Sadia Noorani, Eric Oksenhendler, Mark Ponsford, Waseem Qasim, Isabella Quinti, Alex Richter, Crina Samarghitean, Ravishankar Sargur, Sinisa Savic, Suranjith Seneviratne, Carrock Sewell, Emily Staples, Hans Stauss, James Thaventhiran, Moira Thomas, Steve Welch, Lisa Willcocks, Nigel Yeatman, Patrick Yong, Phil Ancliff, Christian Babbs, Mark Layton, Eleni Louka, Simon McGowan, Adam Mead, Noémi Roy, Jenny Chambers, Peter Dixon, Cecelia Estiu, Bill Hague, Hanns-Ulrich Marschall, Michael Simpson, Sam Chong, Ingrid Emmerson, Lionel Ginsberg, David Gosal, Rob Hadden, Rita Horvath, Mohamed Mahdi-Rogers, Adnan Manzur, Andrew Marshall, Emma Matthews, Mark McCarthy, Mary Reilly, Tara Renton, Andrew Rice, Andreas Themistocleous, Tom Vale, Natalie Van Zuydam, Suellen Walker, Liz Ormondroyd, Gavin Hudson, Wei Wei, Patrick Yu Wai Man, James Whitworth, Maryam Afzal, Elizabeth Colby, Moin Saleem, Omid S. Alavijeh, H. Terry Cook, Sally Johnson, Adam P. Levine, Edwin K.S. Wong, and Rhea Tan.

The project was selected for analysis by the Care4Rare Consortium Gene Discovery Steering Committee, consisting of Kym Boycott, Alex MacKenzie, Jacek Majewski, Michael Brudno, Dennis Bulman, and David Dyment.

Acknowledgments

We thank the four affected individuals involved in this study and their families. This work was supported by the Cambridge Biomedical Research Centre and the National Institute for Health Research (NIHR) for the NIHR BioResource (grant number RG65966). This work was supported by the Care4Rare Canada Consortium (Enhanced Care for Rare Genetic Diseases in Canada), which is funded by Genome Canada, the Canadian Institutes of Health Research, the Ontario Genomics Institute, the Ontario Research Fund, Genome Quebec, and the Children's Hospital of Eastern Ontario Foundation.

Declaration of Interests

The authors declare no competing interests.

Received: March 12, 2018
Accepted: June 4, 2018
Published: June 28, 2018

Web Resources

Ensembl, https://useast.ensembl.org/index.html
ExAC Browser, http://exac.broadinstitute.org/
GenBank, https://www.ncbi.nlm.nih.gov/genbank/
gnomAD, http://gnomad.broadinstitute.org/
Matchmaker Exchange, http://www.matchmakerexchange.org/
OMIM, http://omim.org/

References

1. Vissers, L.E.L.M., Gilissen, C., and Veltman, J.A. (2016). Genetic studies in intellectual disability and related disorders. Nat. Rev. Genet. *17*, 9–18.
2. Martínez, F., Caro-Llopis, A., Roselló, M., Oltra, S., Mayo, S., Monfort, S., and Orellana, C. (2017). High diagnostic yield of syndromic intellectual disability by targeted next-generation sequencing. J. Med. Genet. *54*, 87–92.
3. Veltman, J.A., and Brunner, H.G. (2012). De novo mutations in human genetic disease. Nat. Rev. Genet. *13*, 565–575.
4. Rauch, A., Wieczorek, D., Graf, E., Wieland, T., Endele, S., Schwarzmayr, T., Albrecht, B., Bartholdi, D., Beygo, J., Di Donato, N., et al. (2012). Range of genetic mutations associated with severe non-syndromic sporadic intellectual disability: an exome sequencing study. Lancet *380*, 1674–1682.
5. Hamdan, F.F., Srour, M., Capo-Chichi, J.-M., Daoud, H., Nassif, C., Patry, L., Massicotte, C., Ambalavanan, A., Spiegelman, D., Diallo, O., et al. (2014). De novo mutations in moderate or severe intellectual disability. PLoS Genet. *10*, e1004772.
6. Wilfert, A.B., Sulovari, A., Turner, T.N., Coe, B.P., and Eichler, E.E. (2017). Recurrent de novo mutations in neurodevelopmental disorders: properties and clinical implications. Genome Med. *9*, 101.
7. Deciphering Developmental Disorders Study (2017). Prevalence and architecture of de novo mutations in developmental disorders. Nature *542*, 433–438.
8. Philippakis, A.A., Azzariti, D.R., Beltran, S., Brookes, A.J., Brownstein, C.A., Brudno, M., Brunner, H.G., Buske, O.J., Carey, K., Doll, C., et al. (2015). The Matchmaker Exchange: a platform for rare disease gene discovery. Hum. Mutat. *36*, 915–921.
9. Beaulieu, C.L., Majewski, J., Schwartzentruber, J., Samuels, M.E., Fernandez, B.A., Bernier, F.P., Brudno, M., Knoppers, B., Marcadier, J., Dyment, D., et al.; FORGE Canada Consortium (2014). FORGE Canada Consortium: outcomes of a 2-year national rare-disease gene-discovery project. Am. J. Hum. Genet. *94*, 809–817.
10. Carss, K.J., Arno, G., Erwood, M., Stephens, J., Sanchis-Juan, A., Hull, S., Megy, K., Grozeva, D., Dewhurst, E., Malka, S., et al.; NIHR-BioResource Rare Diseases Consortium (2017). Comprehensive Rare Variant Analysis via Whole-Genome Sequencing to Determine the Molecular Pathology of Inherited Retinal Disease. Am. J. Hum. Genet. *100*, 75–90.
11. Lek, M., Karczewski, K.J., Minikel, E.V., Samocha, K.E., Banks, E., Fennell, T., O'Donnell-Luria, A.H., Ware, J.S., Hill, A.J., Cummings, B.B., et al.; Exome Aggregation Consortium (2016). Analysis of protein-coding genetic variation in 60,706 humans. Nature *536*, 285–291.
12. Dahl, J.P., Wang-Dunlop, J., Gonzales, C., Goad, M.E.P., Mark, R.J., and Kwak, S.P. (2003). Characterization of the WAVE1 knock-out mouse: implications for CNS development. J. Neurosci. *23*, 3343–3352.
13. Auton, A., Brooks, L.D., Durbin, R.M., Garrison, E.P., Kang, H.M., Korbel, J.O., Marchini, J.L., McCarthy, S., McVean, G.A., Abecasis, G.R.; and 1000 Genomes Project Consortium (2015). A global reference for human genetic variation. Nature *526*, 68–74.
14. Stradal, T.E.B., Rottner, K., Disanza, A., Confalonieri, S., Innocenti, M., and Scita, G. (2004). Regulation of actin dynamics by WASP and WAVE family proteins. Trends Cell Biol. *14*, 303–311.
15. Lelieveld, S.H., Wiel, L., Venselaar, H., Pfundt, R., Vriend, G., Veltman, J.A., Brunner, H.G., Vissers, L.E.L.M., and Gilissen, C. (2017). Spatial Clustering of de Novo Missense Mutations Identifies Candidate Neurodevelopmental Disorder-Associated Genes. Am. J. Hum. Genet. *101*, 478–484.
16. Chen, Z., Borek, D., Padrick, S.B., Gomez, T.S., Metlagel, Z., Ismail, A.M., Umetani, J., Billadeau, D.D., Otwinowski, Z., and Rosen, M.K. (2010). Structure and control of the actin regulatory WAVE complex. Nature *468*, 533–538.

17. Padrick, S.B., Cheng, H.-C., Ismail, A.M., Panchal, S.C., Doolittle, L.K., Kim, S., Skehan, B.M., Umetani, J., Brautigam, C.A., Leong, J.M., and Rosen, M.K. (2008). Hierarchical regulation of WASP/WAVE proteins. Mol. Cell *32*, 426–438.
18. Padrick, S.B., Doolittle, L.K., Brautigam, C.A., King, D.S., and Rosen, M.K. (2011). Arp2/3 complex is bound and activated by two WASP proteins. Proc. Natl. Acad. Sci. USA *108*, E472–E479.
19. Nagy, E., and Maquat, L.E. (1998). A rule for termination-codon position within intron-containing genes: when nonsense affects RNA abundance. Trends Biochem. Sci. *23*, 198–199.
20. Suetsugu, S., Yamazaki, D., Kurisu, S., and Takenawa, T. (2003). Differential roles of WAVE1 and WAVE2 in dorsal and peripheral ruffle formation for fibroblast cell migration. Dev. Cell *5*, 595–609.
21. Yamazaki, D., Fujiwara, T., Suetsugu, S., and Takenawa, T. (2005). A novel function of WAVE in lamellipodia: WAVE1 is required for stabilization of lamellipodial protrusions during cell spreading. Genes Cells *10*, 381–392.
22. Takenawa, T., and Miki, H. (2001). WASP and WAVE family proteins: key molecules for rapid rearrangement of cortical actin filaments and cell movement. J. Cell Sci. *114*, 1801–1809.
23. Sung, J.Y., Engmann, O., Teylan, M.A., Nairn, A.C., Greengard, P., and Kim, Y. (2008). WAVE1 controls neuronal activity-induced mitochondrial distribution in dendritic spines. Proc. Natl. Acad. Sci. USA *105*, 3112–3116.
24. Vanstone, J.R., Smith, A.M., McBride, S., Naas, T., Holcik, M., Antoun, G., Harper, M.-E., Michaud, J., Sell, E., Chakraborty, P., et al.; Care4Rare Consortium (2016). DNM1L-related mitochondrial fission defect presenting as refractory epilepsy. Eur. J. Hum. Genet. *24*, 1084–1088.
25. Kosmicki, J.A., Samocha, K.E., Howrigan, D.P., Sanders, S.J., Slowikowski, K., Lek, M., Karczewski, K.J., Cutler, D.J., Devlin, B., Roeder, K., et al. (2017). Refining the role of de novo protein-truncating variants in neurodevelopmental disorders by using population reference samples. Nat. Genet. *49*, 504–510.
26. Bellus, G.A., Hefferon, T.W., Ortiz de Luna, R.I., Hecht, J.T., Horton, W.A., Machado, M., Kaitila, I., McIntosh, I., and Francomano, C.A. (1995). Achondroplasia is defined by recurrent G380R mutations of FGFR3. Am. J. Hum. Genet. *56*, 368–373.
27. Hood, R.L., Lines, M.A., Nikkel, S.M., Schwartzentruber, J., Beaulieu, C., Nowaczyk, M.J.M., Allanson, J., Kim, C.A., Wieczorek, D., Moilanen, J.S., et al.; FORGE Canada Consortium (2012). Mutations in SRCAP, encoding SNF2-related CREBBP activator protein, cause Floating-Harbor syndrome. Am. J. Hum. Genet. *90*, 308–313.
28. Hamdan, F.F., Myers, C.T., Cossette, P., Lemay, P., Spiegelman, D., Laporte, A.D., Nassif, C., Diallo, O., Monlong, J., Cadieux-Dion, M., et al.; Deciphering Developmental Disorders Study (2017). High Rate of Recurrent De Novo Mutations in Developmental and Epileptic Encephalopathies. Am. J. Hum. Genet. *101*, 664–685.
29. Miki, H., Suetsugu, S., and Takenawa, T. (1998). WAVE, a novel WASP-family protein involved in actin reorganization induced by Rac. EMBO J. *17*, 6932–6941.
30. Chen, B., Chou, H.-T., Brautigam, C.A., Xing, W., Yang, S., Henry, L., Doolittle, L.K., Walz, T., and Rosen, M.K. (2017). Rac1 GTPase activates the WAVE regulatory complex through two distinct binding sites. eLife *6*, 6.
31. Kunda, P., Craig, G., Dominguez, V., and Baum, B. (2003). Abi, Sra1, and Kette control the stability and localization of SCAR/WAVE to regulate the formation of actin-based protrusions. Curr. Biol. *13*, 1867–1875.
32. Reijnders, M.R.F., Ansor, N.M., Kousi, M., Yue, W.W., Tan, P.L., Clarkson, K., Clayton-Smith, J., Corning, K., Jones, J.R., Lam, W.W.K., et al.; Deciphering Developmental Disorders Study (2017). RAC1 Missense Mutations in Developmental Disorders with Diverse Phenotypes. Am. J. Hum. Genet. *101*, 466–477.
33. Jaworski, J., Kapitein, L.C., Gouveia, S.M., Dortland, B.R., Wulf, P.S., Grigoriev, I., Camera, P., Spangler, S.A., Di Stefano, P., Demmers, J., et al. (2009). Dynamic microtubules regulate dendritic spine morphology and synaptic plasticity. Neuron *61*, 85–100.
34. Fischer, M., Kaech, S., Knutti, D., and Matus, A. (1998). Rapid actin-based plasticity in dendritic spines. Neuron *20*, 847–854.
35. van Bokhoven, H. (2011). Genetic and epigenetic networks in intellectual disabilities. Annu. Rev. Genet. *45*, 81–104.
36. Pilpel, Y., and Segal, M. (2005). Rapid WAVE dynamics in dendritic spines of cultured hippocampal neurons is mediated by actin polymerization. J. Neurochem. *95*, 1401–1410.
37. Soderling, S.H., Guire, E.S., Kaech, S., White, J., Zhang, F., Schutz, K., Langeberg, L.K., Banker, G., Raber, J., and Scott, J.D. (2007). A WAVE-1 and WRP signaling complex regulates spine density, synaptic plasticity, and memory. J. Neurosci. *27*, 355–365.
38. Kim, Y., Sung, J.Y., Ceglia, I., Lee, K.-W., Ahn, J.-H., Halford, J.M., Kim, A.M., Kwak, S.P., Park, J.B., Ho Ryu, S., et al. (2006). Phosphorylation of WAVE1 regulates actin polymerization and dendritic spine morphology. Nature *442*, 814–817.
39. Hazai, D., Szudoczki, R., Ding, J., Soderling, S.H., Weinberg, R.J., Sótonyi, P., and Rácz, B. (2013). Ultrastructural abnormalities in CA1 hippocampus caused by deletion of the actin regulator WAVE-1. PLoS ONE *8*, e75248.
40. Soderling, S.H., Langeberg, L.K., Soderling, J.A., Davee, S.M., Simerly, R., Raber, J., and Scott, J.D. (2003). Loss of WAVE-1 causes sensorimotor retardation and reduced learning and memory in mice. Proc. Natl. Acad. Sci. USA *100*, 1723–1728.
41. Law, R., Dixon-Salazar, T., Jerber, J., Cai, N., Abbasi, A.A., Zaki, M.S., Mittal, K., Gabriel, S.B., Rafiq, M.A., Khan, V., et al. (2014). Biallelic truncating mutations in FMN2, encoding the actin-regulatory protein Formin 2, cause nonsyndromic autosomal-recessive intellectual disability. Am. J. Hum. Genet. *95*, 721–728.
42. Rivière, J.-B., van Bon, B.W.M., Hoischen, A., Kholmanskikh, S.S., O'Roak, B.J., Gilissen, C., Gijsen, S., Sullivan, C.T., Christian, S.L., Abdul-Rahman, O.A., et al. (2012). De novo mutations in the actin genes ACTB and ACTG1 cause Baraitser-Winter syndrome. Nat. Genet. *44*, 440–444, S1–S2.
43. Kutsche, K., Yntema, H., Brandt, A., Jantke, I., Nothwang, H.G., Orth, U., Boavida, M.G., David, D., Chelly, J., Fryns, J.P., et al. (2000). Mutations in ARHGEF6, encoding a guanine nucleotide exchange factor for Rho GTPases, in patients with X-linked mental retardation. Nat. Genet. *26*, 247–250.
44. Yan, Y., Tsukamoto, O., Nakano, A., Kato, H., Kioka, H., Ito, N., Higo, S., Yamazaki, S., Shintani, Y., Matsuoka, K., et al. (2015). Augmented AMPK activity inhibits cell migration by phosphorylating the novel substrate Pdlim5. Nat. Commun. *6*, 6137.
45. Li, Z., Okamoto, K., Hayashi, Y., and Sheng, M. (2004). The importance of dendritic mitochondria in the morphogenesis and plasticity of spines and synapses. Cell *119*, 873–887.

The American Journal of Human Genetics, Volume *103*

Supplemental Data

De Novo Truncating Mutations in *WASF1* Cause Intellectual Disability with Seizures

Yoko Ito, Keren J. Carss, Sofia T. Duarte, Taila Hartley, Boris Keren, Manju A. Kurian, Isabelle Marey, Perinne Charles, Carla Mendonça, Caroline Nava, Rolph Pfundt, Alba Sanchis-Juan, Hans van Bokhoven, Anthony van Essen, Conny van Ravenswaaij-Arts, NIHR BioResource, Care4Rare Canada Consortium, Kym M. Boycott, Kristin D. Kernohan, Sarah Dyack, and F. Lucy Raymond

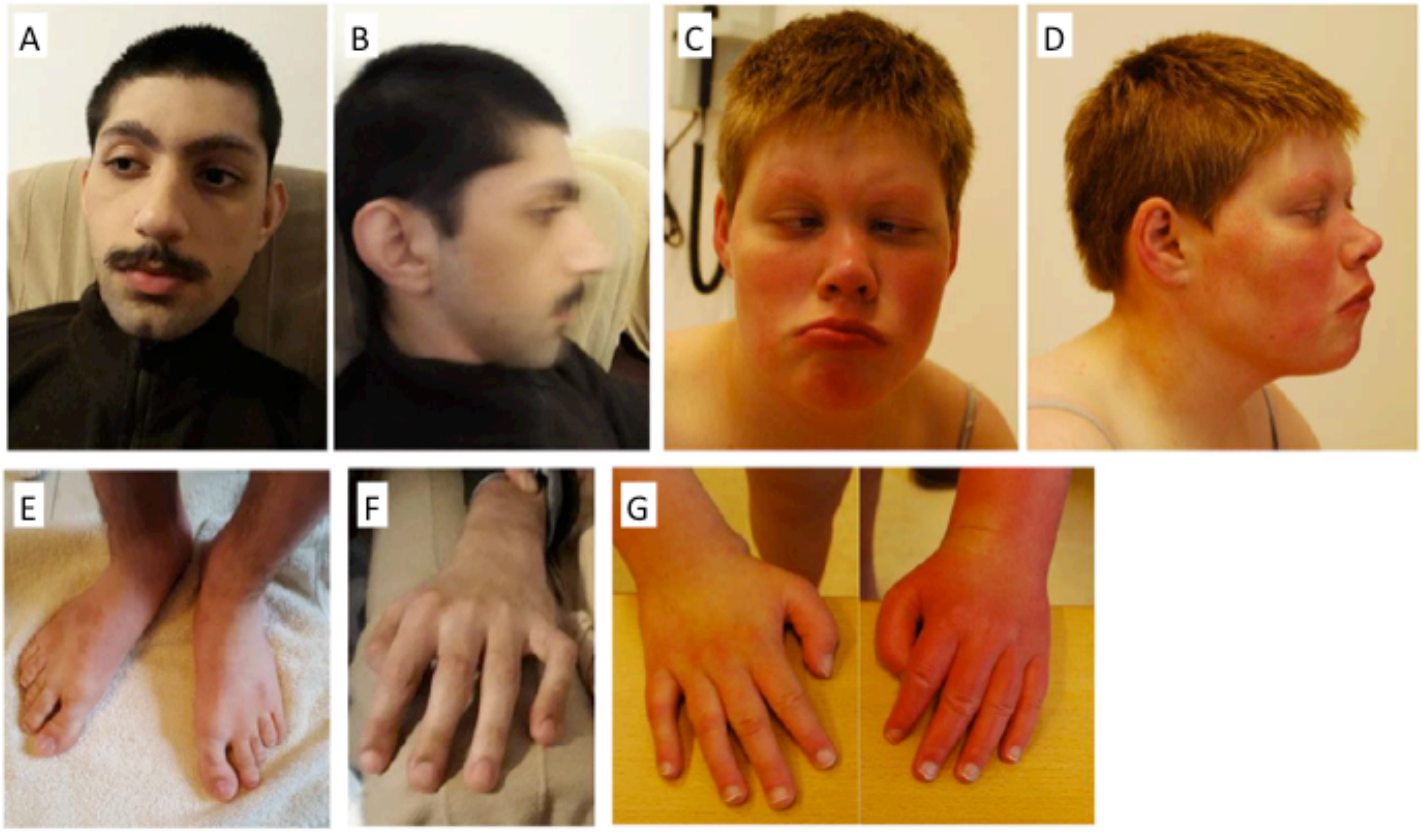

Figure S1. Clinical phenotype of affected individuals. (A-B) Facial phenotype of P3 with midface hypoplasia. (C-D) Facial phenotype of P4 with strabismus. (E) Foot morphology of P1 showing pes planus and bilateral short 4th toes. (F) Hand morphology of P3 with arachnodactyly. (G) Normal hand morphology of P4.

A

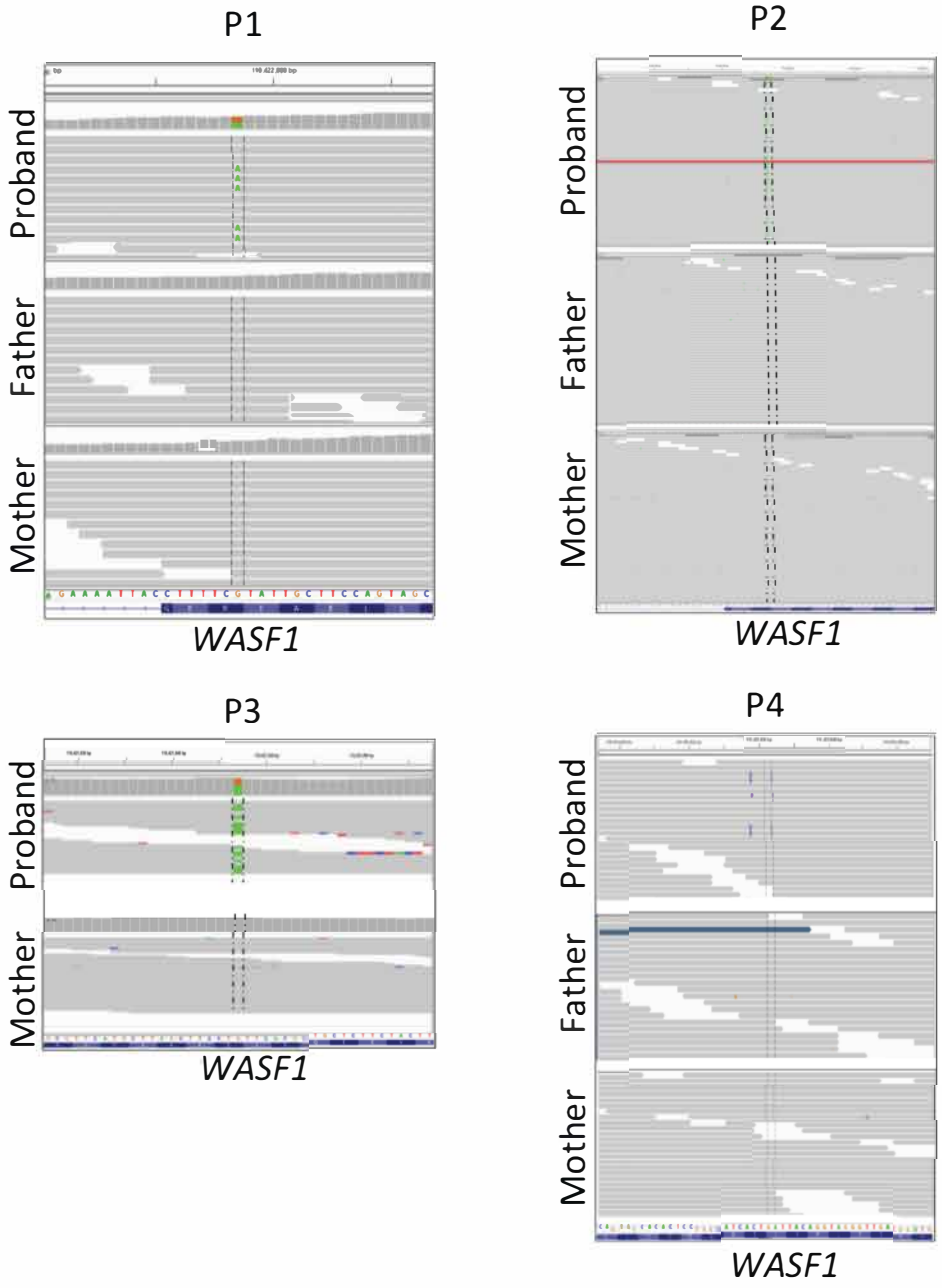
P1
Proband
Father
Mother
WASF1
P2
Proband
Father
Mother
WASF1
P3
Proband
Mother
WASF1
P4
Proband
Father
Mother
WASF1

B

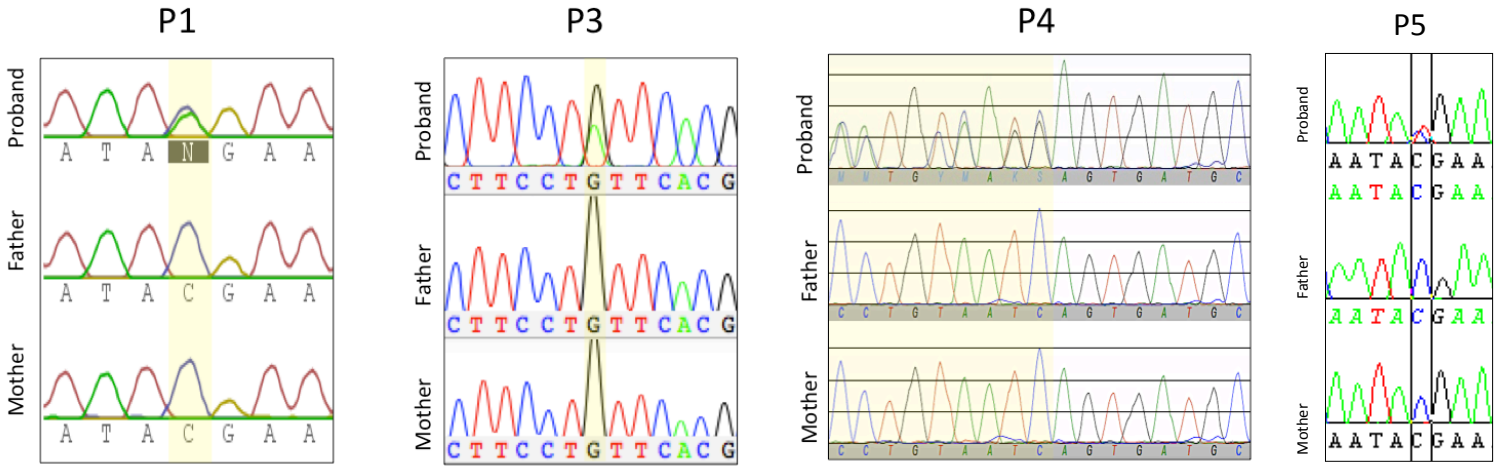

Figure S2. Confirmation of *WASF1* mutations. P1, P2 and P5 have 6:g.110422797G>A; P3 has 6:g.110421847G>A; P4 has 6:g.110422831delinsCCTGGC. **A)** Integrated Genomics Viewer plots show high-throughput sequencing reads in four affected individuals. **B)** Sanger confirmations of P1, P3, P4 and P5 trios.

A

Cells With Lamellipodia Only

Cells With Both Lamellipodia and Filopodia

Cells With Filopodia Only

Cellular phenotype severity

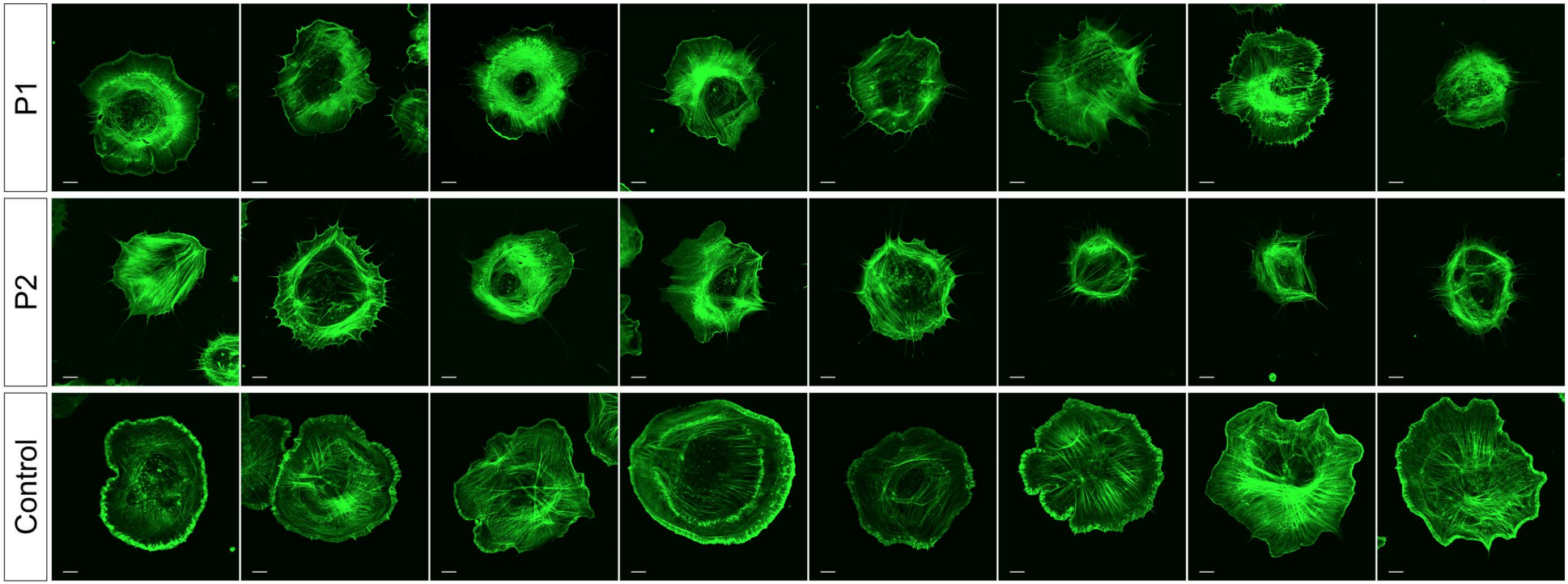

B

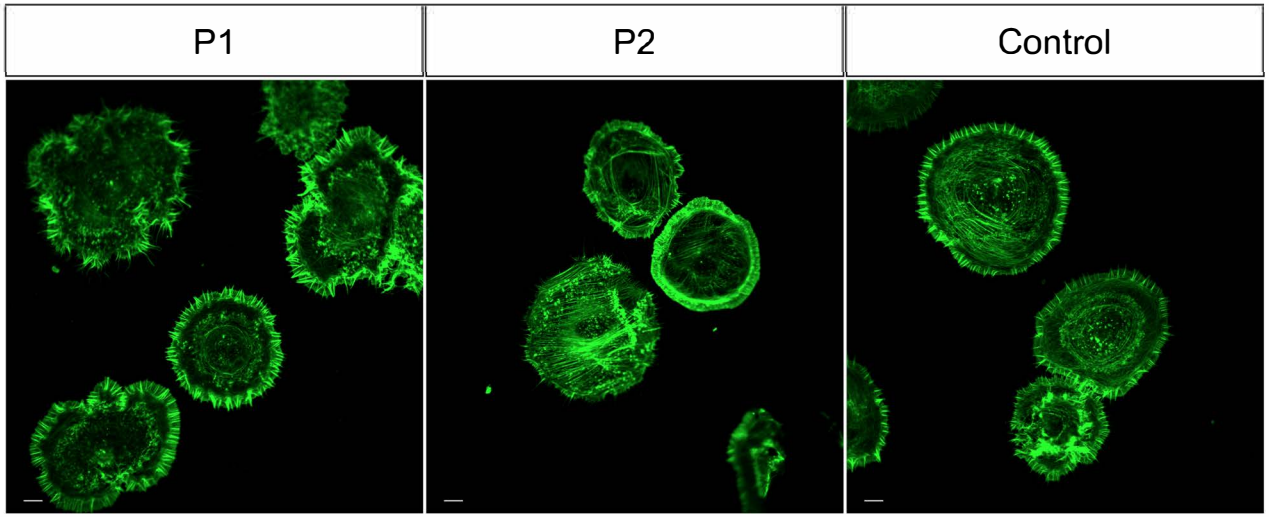

Figure S3. Morphology of fibroblasts.

Range in actin morphology in fibroblasts derived from individuals with the c.1516C>T variant. Actin was visualized in PDGF-induced fibroblasts by staining with phalloidin. (A) Representative cells from P1, P2, and control fibroblasts showing the diversity in cell phenotype. Scale bars are 10μm. (B) Field of view image of phalloidin-stained cells. Scale bars are 10μm.

Table S1. Method details.

Individual	Sequencing	Alignment	Data	Variant callers	Structural variants considered
P1	SureSelect All Exon 50 Mb library preparation (Agilent) followed by sequencing on an Illumina HiSeq 2000.	Burrows-Wheeler Aligner.[1]	100bps paired-end reads with a median coverage of targeted regions of 140X.	SAMtools.[2]	No
P2 and P5	MedExome library preparation (Roche), followed by Illumina NextSeq high output sequencing.	Burrows-Wheeler Aligner.	150bps paired-end reads with a median coverage of targeted regions of 142X.	Genome Analyzer Toolkit.	No
P3	TruSeq DNA PCR-Free library preparation (Illumina), followed by whole genome sequencing on an Illumina HiSeq X Ten.	Isaac aligner.[3]	150bps paired-end reads with a median coverage genome-wide of 36X.	Isaac variant caller, Canvas, and Manta.[3–5]	Yes
P4	SureSelectXT Human All Exon 50Mb library preparation (Agilent), followed by sequencing on an Illumina HiSeq 2000.	Burrows-Wheeler Aligner.	Short reads with a median coverage genome-wide of 75X.	Genome Analyzer Toolkit.	Yes

Table S2: Variants of unknown significance in individuals with *WASF1* mutations. Genomic coordinates refer to GRCh37. NR = none reported. XLID = X-linked intellectual disability.

Individual	Gene	Variant (HGVSg)	Variant (HGVSc)	Variant (HGVSp)	Predicted Consequence	CADD (phred scaled)	Genotype	Inheritance	gnomAD frequency	In ClinVar	Confirmed by Sanger sequencing	Disease associated with gene	Comments
P1	*ATP5J*	21:g.27101990 T>C	ENST00000400093.3:c.116T>C	ENSP00000284971.3:p.Iso39Thr	Missense	15	Het	*De novo*	0	No	Yes	NR	Gene not constrained for LOF or missense variation in ExAC. Encodes a subunit of the H+ ATP synthase complex, Iso39 is poorly conserved between species.
P1	*SLC38A4*	12:g.47163175 C>T	ENST00000266579.8:c.1136C>T	ENSP00000266579.4:p.Arg446Ter	Stop Gain	NA	Het	*De novo*	0	No	Yes	NR	Unlikely candidate because expressed predominantly in the liver.
P1	*ZNF175*	19:g.52091449 A>G	ENST00000262259.6:c.1865A>G	ENSP00000262259.2:p.Lys622Arg	Missense	4.46	Het	*De novo*	4/277122	No	Yes	NR	Unlikely candidate because at least 40 LOF variants occur before this c.1865A>G variant in the gnoMAD database; one of these variants (rs746669166) occurs at an allele frequency of 0.25%. Gene not constrained for LOF or missense

													variation in ExAC.
P1	*CROCC*	1:g.17281987C>T	ENST00000375541.9:c.3646C>T	ENSP00000364691.4:p.Arg1216Trp	Missense	14.33	Het	Inherited from mother	2/189508	No	No	NR	Structural component of ciliary rootlets; unlikely candidate because *CROCC* is a frequently mutated gene with a z-missense score of -0.97 in the ExAC database.
		1:g.17296892C>T	ENST00000375541.9:c.5596C>T	ENSP00000364691.4:p.Arg1866Cys	Missense	21.4	Het	Inherited from father	35/255994	No	No		
P2	*CDCA7L*	7:g.21956404C>T	ENST00000406877.3:c.133G>A	ENSP00000383986.3:p.Asp45Asn	Missense	19	Het	*De novo*	0	No	No	NR	Gene not constrained for LOF or missense variation in ExAC. No outcome in GeneMatcher.
P3	*ACSL4*	X:g.108912393C>T	ENST00000340800.2:c.1135G>A	ENSP00000339787.2:p.Asp379Asn	Missense	29	Hemi	Inherited from unaffected heterozygous mother	3/174894	No	No	XLID	Female carriers of pathogenic *ACSL4* variants have skewed X-inactivation.

Supplemental references

1. Li, H., and Durbin, R. (2009). Fast and accurate short read alignment with Burrows-Wheeler transform. Bioinformatics *25*, 1754–1760.

2. Li, H., Handsaker, B., Wysoker, A., Fennell, T., Ruan, J., Homer, N., Marth, G., Abecasis, G., and Durbin, R. (2009). The Sequence Alignment/Map format and SAMtools. Bioinformatics *25*, 2078–2079.

3. Raczy, C., Petrovski, R., Saunders, C.T., Chorny, I., Kruglyak, S., Margulies, E.H., Chuang, H.Y., Källberg, M., Kumar, S. a., Liao, A., et al. (2013). Isaac: Ultra-fast whole-genome secondary analysis on Illumina sequencing platforms. Bioinformatics *29*, 2041–2043.

4. Chen, X., Schulz-Trieglaff, O., Shaw, R., Barnes, B., Schlesinger, F., Källberg, M., Cox, A.J., Kruglyak, S., and Saunders, C.T. (2015). Manta: rapid detection of structural variants and indels for germline and cancer sequencing applications. Bioinformatics *32*, 1220–1222.

5. Roller, E., Ivakhno, S., Lee, S., Royce, T., and Tanner, S. (2016). Canvas: versatile and scalable detection of copy number variants. Bioinformatics *32*, 2375–2377.